AGU PUBLICATIONS

JGR

Journal of Geophysical Research: Biogeosciences

RESEARCH ARTICLE

10.1002/2014JG002691

This article is a companion to *Fründt et al.* [2015] doi:10.1002/2014JG002692.

Key Points:
- New method is shown to calculate highly resolved Chl fields for past decades
- Resulting Chl field in the Madeira Basin is correlated with NAO
- The method allows estimation of Chl and carbon uptake over last century

Correspondence to:
J. J. Waniek,
joanna.waniek@io-warnemuende.de

Citation:
Fründt, B., J. W. Dippner, and J. J. Waniek (2015), Chlorophyll *a* reconstruction from in situ measurements: 1. Method description, *J. Geophys. Res. Biogeosci.*, *120*, 237–245, doi:10.1002/2014JG002691.

Received 22 APR 2014
Accepted 10 JAN 2015
Accepted article online 28 JAN 2015
Published online 24 FEB 2015

Chlorophyll *a* reconstruction from in situ measurements: 1. Method description

B. Fründt[1], J. W. Dippner[1], and J. J. Waniek[1]

[1]Leibniz-Institute for Baltic Sea Research Warnemünde, Rostock, Germany

Abstract Understanding the development of primary production is essential for projections of the global carbon cycle in the context of climate change. A chlorophyll *a* hindcast that serves as a primary production indicator was obtained by fitting in situ measurements of nitrate, chlorophyll *a*, and temperature. The resulting fitting functions were adapted to a modeled temperature field. The method was applied to observations from the Madeira Basin, in the northeastern part of the oligotrophic North Atlantic Subtropical Gyre and yielded a chlorophyll *a* field from 1989 to 2008 with a monthly resolution validated with remotely measured surface chlorophyll *a* data by SeaWiFS. The chlorophyll *a* hindcast determined with our method resolved the seasonal and interannual variability in the phytoplankton biomass of the euphotic zone as well as the deep chlorophyll maximum. Moreover, it will allow estimation of carbon uptake over long time scales.

1. Introduction

Primary production in the oceans accounts for half of the global carbon fixation, and a large part of this carbon is exported into the intermediate and deep oceans [*Field et al.*, 1998; *Schwab et al.*, 2012]. Long-term changes in the growth conditions of phytoplankton in response to atmospheric forcing or an increase in temperature, as in recent decades [*Levitus et al.*, 2005, 2009], can affect the Earth's climate and the global carbon cycle by changing the amount of carbon fixation [*Denman et al.*, 2007]. Understanding the changes in phytoplankton biomass occurring under climate conditions of the last century will allow robust projections of the global carbon cycle. Studies analyzing long-term variability of primary production have been pursued by *Boyce et al.* [2010] by combining in situ measured chlorophyll *a* data, as primary production indicator, and early measurements of the ocean's transparency to analyze the trend in global primary production from 1899 until 2008. However, deriving primary production from transparency measurements can be affected by large systematical errors producing bias and has therefore been intensively discussed [*Mackas*, 2011; *Rykaczewski and Dunne*, 2011; *McQuatters-Gollop et al.*, 2011; *Boyce et al.*, 2011]. Hence, we introduce a new method to derive chlorophyll *a* hindcasts which is different to that introduced by *Boyce et al.* [2010]. The global decline in chlorophyll *a* since the late 1800s could be related to an increase of upper ocean stratification due to risen sea surface temperatures [*Behrenfeld et al.*, 2006; *Polovina et al.*, 2008]. Methods to measure chlorophyll *a* and primary production in the water column by satellite measurements have been developed [*Sathyendranath et al.*, 1991; *Antoine and Morel*, 1996; *Behrenfeld and Falkowski*, 1997; *Uitz et al.*, 2006] resulting in remotely measured chlorophyll *a* time series by the Coastal Zone Color Scanner from 1976 to 1986 and by SeaWiFS from 1997 until the present [*McClain*, 2009; *Boyce et al.*, 2010].

Contrary to *Boyce et al.* [2010], *Dave and Lozier* [2013] found no significant trend in global chlorophyll *a* in measurements from 1997 until 2010. Furthermore, their previous studies [*Dave and Lozier*, 2010; *Lozier et al.*, 2011] confuted the hypothesis of the negative correlation of ocean stratification and chlorophyll *a* content on interannual time scales especially in the oligotrophic parts of the ocean. The studies by *Chavez et al.* [2011] and *Saba et al.* [2010] also show an increase of primary production in the subtropical gyres of the North Atlantic and North Pacific by analyzing the time series of BATS (Bermuda Atlantic Time series Study) and HOT (Hawaii Ocean Time series) between 1989 and 2007. Nevertheless, the length of both the remotely measured chlorophyll *a* time series and of BATS and HOT are still insufficient to permit an analysis of long-term variability. Within the scope of the two contradictory studies by *Boyce et al.* [2010] and *Dave and Lozier* [2013], it is necessary to devise a new approach for deriving a chlorophyll *a* time series for a time period long enough for detection of long-term trends and variability.

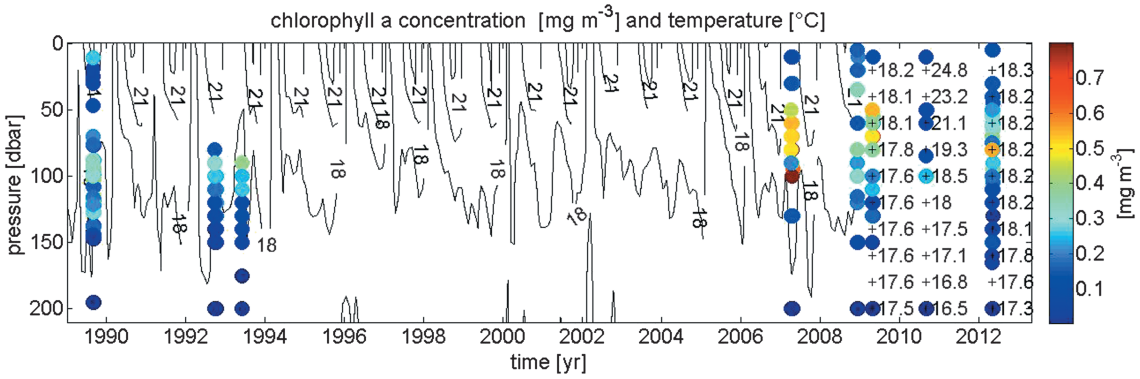

Figure 1. In situ measurements of chlorophyll *a* (1989–2012, colored circles, and color bar) in the Azores Frontal region (29°–38.5°N, 17°–27°W). Isotherms [15, 18, 21, and 24°C] from the simple ocean data assimilation parallel ocean program (SODA POP) temperature field are shown from 1989 to 2008. Between 2009 and 2012, because no SODA POP data were available, temperature was obtained by conductivity-temperature-depth (CTD) (crosses).

Here we present a method to reconstruct the chlorophyll *a* distribution of several past decades. The Madeira Basin, in the North Atlantic Subtropical Gyre, was deemed appropriate as the study area because a continuous record of temperature measurements at the mooring site Kiel276 (33°N, 22°W) has documented a clear temperature increase within the thermocline since 1980 [*Fründt et al.*, 2013]. Although chlorophyll *a* has been sparsely measured in this region (Figure 1), the results of our method will provide better understanding of the consequences of altered environmental conditions for primary production.

2. Data

To reconstruct the chlorophyll *a* field, a correlation of in situ temperature and nitrate measurements was adapted to a modeled temperature field, yielding a nitrate field. Additional in situ chlorophyll *a* data was related to both temperature and nitrate, and their respective fields were used to calculate the chlorophyll *a* field.

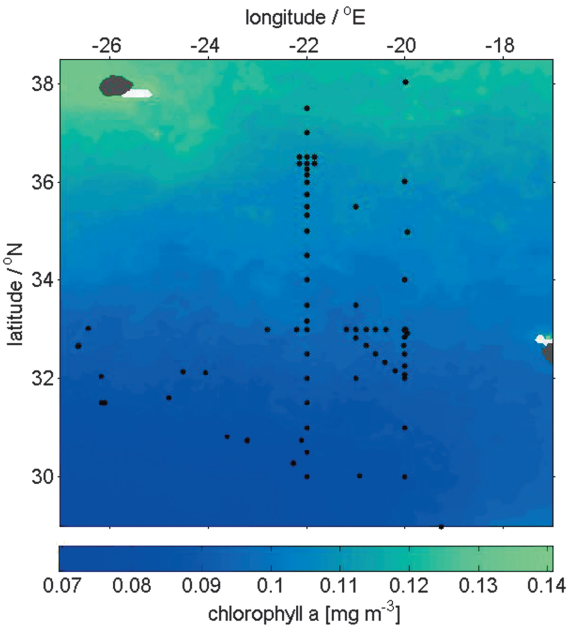

Figure 2. Positions (black dots) of the in situ measurements of temperature, nitrate, and chlorophyll *a* in the Azores Frontal Region (29–38.5°N, 17–27°W) and the mean surface chlorophyll *a* concentrations (indicated by the color bar) from Moderate Resolution Imaging Spectroradiometer (MODIS, average 2003–2011, 9 km resolution).

Given the relatively few measurements of chlorophyll *a* directly at the position of the mooring site Kiel276 (33°N, 22°W), the data set was enlarged with measurements from the Azores Frontal region (29–38.5°N, 17–27°W) [*Fründt and Waniek*, 2012] (Figures 1 and 2). This also served to reduce the effects of patchiness. In situ measurements were taken from different cruises within the Madeira Basin and from data sets of the Pangaea database (http://www.pangaea.de/) (Figure 2 and Table 1). In situ measurements taken near islands were removed from the application because these regions are affected by upwelling at the subsurface island slopes.

Temperature in situ measurements of the cruises with the RV *Poseidon* (Table 1) were taken from calibrated conductivity-temperature-depth (Seabird 911) casts. Nitrate concentrations were measured using an autoanalyzer (EVOLUTION III, Alliance Instruments) according to standard methods [*Grasshoff et al.*, 1999]. The chlorophyll *a* concentration was determined

Table 1. Cruises in the Azores Frontal (AF) Region and Number of In Situ Measurements of Nitrate, When Temperature Data Were Available, and of Chlorophyll *a* (CHL), When Temperature and Nitrate Data Were Available[a]

Cruise / Station Number	Ship	Time of Sampling[b] in AF Zone	Data Points of Nitrate(*T*)	Data Points of CHL (*T*,N)	Reference
NAPP89-1	RV Tyro	28/08–7/9/1989	111	47	*Rommets et al.* [1991a]
NAPP90-1	RV Tyro	28/04–10/5/1990	111	47	*Rommets et al.* [1991b]
HUD92/37	Hudson	24/09–12/10/1992	96	25	*Irwin* [2000]
HUD93/2	Hudson	29/05–30/5/1993	60	19	*Irwin* [2000]
M36/2	Meteor (1996)	23/06–1/7/1996	165	156	*Mienert et al.* [1998]
POS349	Poseidon	09/04–22/4/2007	214	83	*Fründt and Waniek* [2012]
POS377	Poseidon	08/12–13/12/2008	58	38	Waniek et al., Cruise report, unpublished
POS383	Poseidon	22/04–2/5/2009	94	41	Waniek et al., Cruise report, unpublished
POS404	Poseidon	03/09–8/9/2010	74	40	*Waniek* [2010]
POS432	Poseidon	03/05–10/5/2012	210	73	Krüger et al., Cruise report[c]

[a]Both were used to calculate chlorophyll *a* on 33°N, 22°W.
[b]Dates in the third column are formatted as day/month/year.
[c]Provided at http://www.geomar.de/en/centre/central-facilities/wasser/f-s-poseidon/.

with a fluorometer (TURNER 10-AU, Gamma Analysen Technik GmbH) calibrated using the *Protocols for the Joint Global Ocean Flux Study (JGOFS) core measurements* [1994].

The modeled temperature field was the output of the Simple Ocean Data Assimilation Parallel Ocean Program (SODA POP) [*Carton et al.*, 2005; *Carton and Giese*, 2008] version 2.1.6 for 33.2°N, 22.2°W (available at http://apdrc.soest.hawaii.edu/datadoc/soda_2.1.6.php).

For validation, satellite chlorophyll *a* measurements in the Madeira Basin, made by SeaWiFS with an 8 day resolution between 29 August 1997 and 18 December 2010, were used. It has to be noted that these satellite measurements include an RMS error of up to 28% in the open ocean [*Gregg and Casey*, 2004]. The data set is freely available at http://gdata1.sci.gsfc.nasa.gov/daac-bin/G3/gui.cgi?instance_id=ocean_8day.

The impact of atmospheric long-term changes is discussed using the winter North Atlantic Oscillation (NAO) index from December to March (freely available at https://climatedataguide.ucar.edu/ and *Hurrell* [1995]).

3. Methods

The euphotic depth was either derived from the Secchi depth or calculated using the exponential law of light attenuation [*Kirk*, 2011]. In our case, the depth of the euphotic layer Z_{eu} varied between 93 m (derived from Secchi depth) and 153 m (calculated after *Kirk* [2011]), depending on the integrated chlorophyll *a* content in the overlying water column:

$$Z_{eu}(\mathrm{CHL_{int}})\,[\mathrm{m}] = -1.7\ \mathrm{m^3\ mg^{-1}} \cdot \mathrm{CHL_{int}}\ [\mathrm{mg\ m^{-2}}] + 160\ \mathrm{m} \quad (1)$$

with $\mathrm{CHL_{int}}$ the vertical integrated chlorophyll *a* concentration.

Three steps were required to determine the chlorophyll *a* hindcast (Figure 3): In the first step, it was assumed that primary production in the Madeira Basin is nitrate-limited [*Mills et al.*, 2004], and no distinction between different phytoplankton species was made. The correlation between temperature, nitrate, and chlorophyll *a* was considered as conservative, i.e., at a given temperature and nitrate concentration, the chlorophyll *a* concentration was the same over time. For the temperature field, data from SODA POP at the position of Kiel276 were extracted and the minimum and maximum euphotic depths were determined by Secchi depths or by calculation after the method of *Kirk* [2011]. In the second step, in situ nitrate measurements were fitted to the temperature values after the removal of outliers (Figure 3a), yielding the Gaussian first-order equation:

$$f_1 = \mathrm{Nitrate}(T) = 17.01 \cdot \exp(-((T - 6.45)/6.36)^2) \quad (2)$$

with $R^2 = 0.72$. For error estimation, two additional fits were calculated with the enveloping data points (Figure 3a). Equation (2) was applied to each point of the temperature field resulting in a nitrate field (Figure 3b).

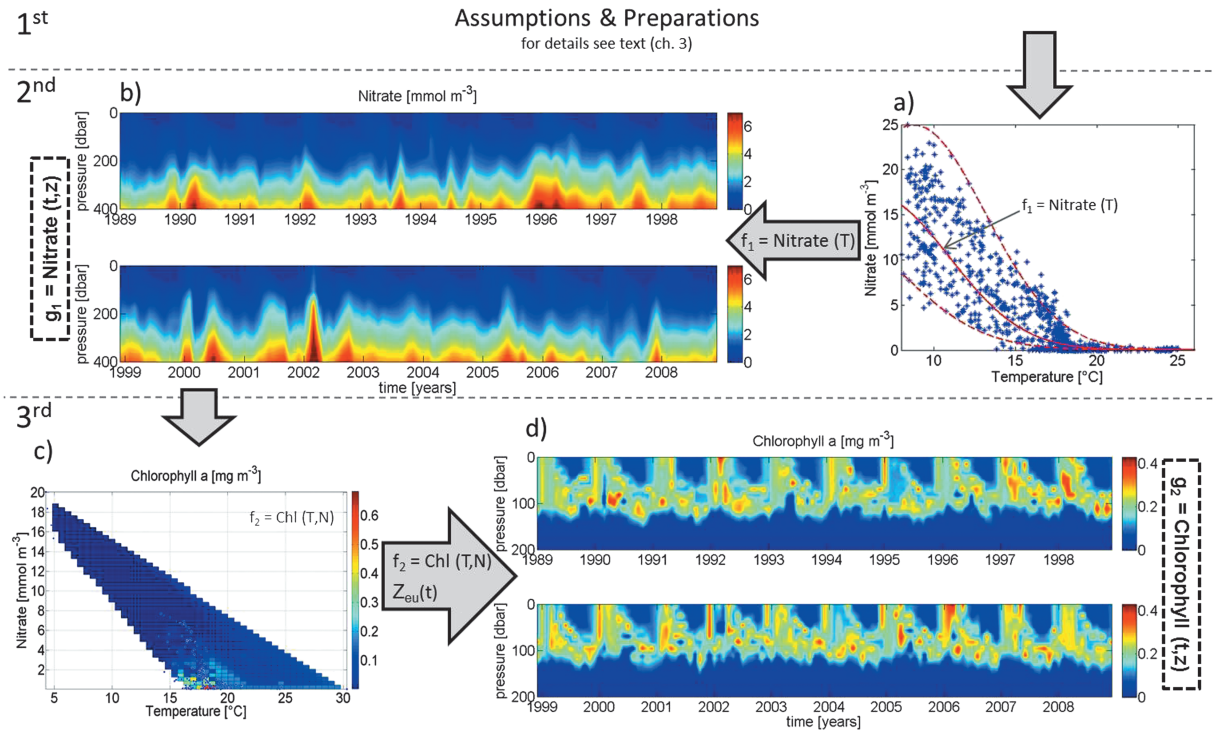

Figure 3. Schema of the method to calculate the past chlorophyll *a* distribution. In the first step, assumptions are established and the data sets are prepared. In the second step, the nitrate field $g_1(t,z)$ is calculated using the fitting function $f_1(T)$. (a) In situ nitrate measurements with respect to temperature (blue stars) and the fitting function f_1 (red line). For error estimation, the lower and upper envelopes (red dashed lines) are given. (b) The calculated nitrate field g_1 = Nitrate(t,z) in the upper 400 m from 1989 to 2008. In the third step, the chlorophyll *a* field $g_2(t,z)$ is calculated using the fitting function $f_2(T,N)$ and the euphotic depth $Z_{eu}(t)$. (c) In situ measurements of chlorophyll *a* with respect to temperature and nitrate (blue circles) and the linear surface fit f_2. (d) The resulting vertically resolved chlorophyll *a* hindcast $g_2(t,z)$ in the upper 200 m from 1989 to 2008.

In the third step, the chlorophyll *a* concentrations measured in situ were surface fitted to both temperature and nitrate (Figure 3c). A piecewise linear surface interpolation (MATLAB, fittype *linearinterp*) was used, yielding the interpolant f_2 = CHL(*T*,N). Next, the temperature and nitrate fields were applied to f_2, resulting in a first chlorophyll *a* hindcast. The euphotic depth $Z_{eu}(t)$ was calculated for each time step and used to remove the overshooting of chlorophyll *a* at higher depths because of the increase in nitrate. By applying $Z_{eu}(t)$ to the first chlorophyll *a* hindcast, the final chlorophyll *a* hindcast was obtained (Figure 3d).

To determine the skill factor of the method, the Nash-Sutcliffe coefficient of efficiency (*E*) [*Nash and Sutcliffe*, 1970; *Legates and McCabe*, 1999] was calculated. Because the time series of the calculated chlorophyll *a* was not normally distributed, the data were first log transformed and standardized. *E* was then calculated as follows:

$$E = 1 - \frac{\sum_i (S_i - M_i)^2}{\sum_i (S_i - \bar{S})^2} \tag{3}$$

where *S* is the satellite-measured data, $\bar{S}$ the mean of *S*, and *M* the chlorophyll *a* data calculated with our method. An efficiency of 1 ($E = 1$) corresponds to a perfect match between the calculated and the remotely measured data. An efficiency of 0 ($E = 0$) indicates that the variance of the calculated chlorophyll *a* is of the same size as the variance of the remotely measured data. Equation (3) is identical with the Brier-based skill score [*Livezey*, 1995].

For discussion, the chlorophyll *a* field is standardized, resulting in a zero mean value and unit variance for each depth. To examine the dominant patterns of the resulting chlorophyll *a* field, empirical orthogonal function (EOF) analysis was calculated with annual mean profiles [*von Storch and Zwiers*, 1999]. Identifying the periods on which the time coefficients behave concurrent to the NAO, wavelet coherences and phase differences were calculated by applying a complex Morlet wavelet ($\omega_0 = 6$) as mother wavelet [*Torrence and Compo*, 1998; *Grinsted et al.*, 2004].

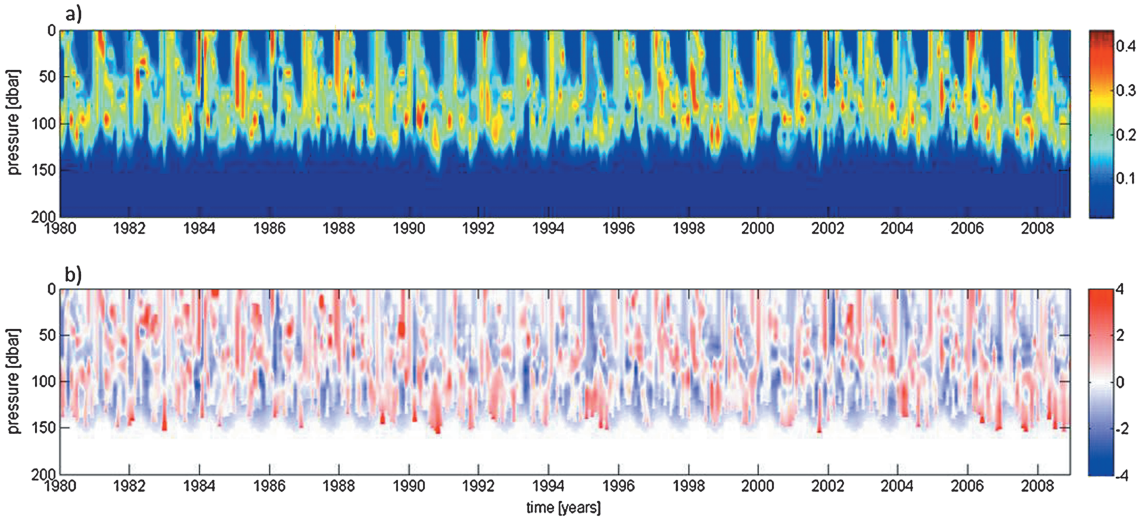

Figure 4. (a) The chlorophyll *a* hindcast (mg m^{-3}) and (b) the standardized chlorophyll *a* hindcast from 1980 to 2008. Note that the standardized chlorophyll *a* hindcast has no units.

4. Results

The method was applied to obtain a chlorophyll *a* hindcast from 1980 to 2008, the same time period, in which in situ measurements from the mooring site Kiel276 demonstrate a marked temperature increase especially in the last decade [*Fründt et al.*, 2013]. The signal was dominated by the phytoplankton bloom from approximately December to March and was confined to the bottom of the euphotic layer until the new bloom developed (Figure 4a), reproducing the deep chlorophyll maximum (DCM). The maximum chlorophyll *a* concentration was found in a mean depth of 70 $\pm$ 40 m, indicating the DCM as dominant feature in the months after the bloom.

Because the calculation of the chlorophyll *a* hindcast is independent from satellite-based chlorophyll *a* measurements, the calculated surface chlorophyll *a* was compared to the remotely measured data for validation (Figure 5). The mean surface chlorophyll *a* concentration (0.14 $\pm$ 0.09 mg m^{-3}) was similar to that determined by satellite measurements (0.12 $\pm$ 0.06 mg m^{-3}). The chlorophyll *a* hindcast reproduced the beginning and the end of the phytoplankton bloom but did not exactly match the interannual variability. The Nash-Sutcliffe coefficient of efficiency [*Nash and Sutcliffe*, 1970; *Legates and McCabe Jr.* 1999] resulted in a value of $E = 0.3$ indicating the method's relatively high capacity to reconstruct the seasonal to long-term variability of the chlorophyll *a* field, since 30% of the natural variability was explained by the hindcasted chlorophyll *a* data. Additionally, this result is revealed in the Pearson's correlation coefficient of 0.65 which was calculated using the log-transformed and standardized time series.

The comparison of calculated chlorophyll *a* and in situ measured chlorophyll a profiles from two cruises in 1989 and 2007 shows that the calculated chlorophyll *a* reproduces well the depth distribution of

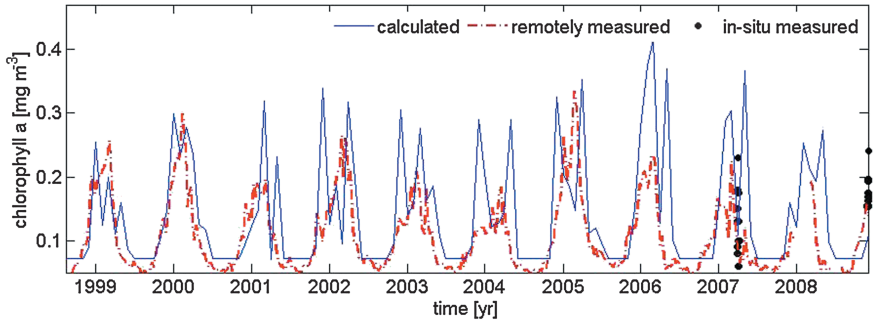

Figure 5. Validation of the calculated chlorophyll *a* concentration (blue solid line) using the surface chlorophyll *a* concentration measured remotely (red dash-dotted line). In situ (black circles) measured surface chlorophyll *a* is also given.

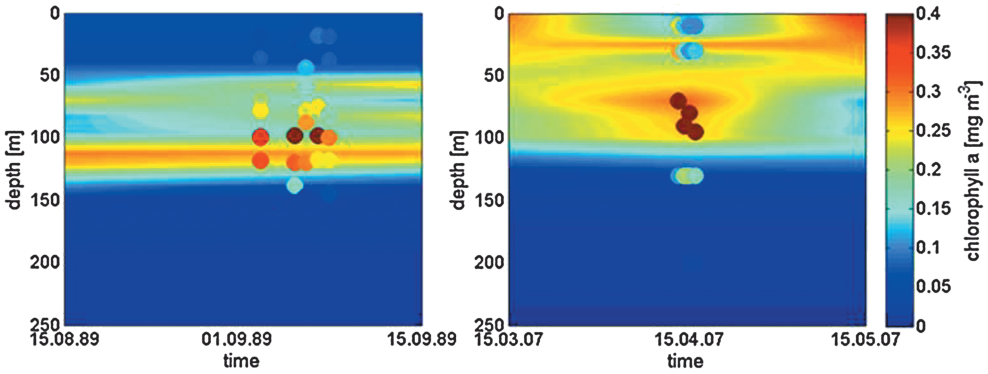

Figure 6. Comparison of the calculated chlorophyll *a* (colored background, in monthly resolution) and in situ measured chlorophyll *a* profiles (colored circles) from two cruises in (left) 1989 (NAPP89-1) and in (right) 2007 (POS349).

chlorophyll *a* including the DCM (Figure 6). A validation with these profiles is not possible because the calculated and in situ measured data are not independent.

The distinct was found nearly all year and extended within the water column over a depth of roughly 50 m around a mean depth of approximately 100 m. The chlorophyll *a* concentration is typically low in the oligotrophic regions, with values of 0.2–0.3 mg m^{-3}. Single events, lasting 1 to 2 months, showed enhanced values of up to 0.45 mg m^{-3}. This intensification mostly occurred within the DCM spanning only few meters. In some years like 1984, 1985, and 1988, strong phytoplankton growth events spanned nearly over the entire euphotic zone (Figure 4a).

Because the chlorophyll *a* field held a high seasonal variability, it was standardized with a mean annual field (Figure 4b). From this approach arose the opportunity for detecting variability of chlorophyll *a* concentrations differing from the mean annual cycle. The standardized chlorophyll *a* field was then used to calculate the EOFs and their time coefficients (Figure 7a). The first EOF explained 55.5% and the second EOF 14.2% of the variability. The time coefficients of both EOFs showed a high interannual variability (Figure 7b).

5. Discussion

The first and second EOFs, together explaining nearly 70% of the variability of the chlorophyll *a* hindcast, emphasized the DCM as the dominant pattern of the chlorophyll *a* field (Figure 7a). Therefore, understanding the interannual variability of the DCM is highly important for an understanding of the chlorophyll *a* development in the entire euphotic zone. Pronounced DCMs were found at the beginning of the time series 1982/1983, from 1989 to 1991, 1995, and at the end of the time series from 2006 to 2008 (Figure 4b). The same periods were characterized by positive NAO indices (Figure 7b). Less distinct DCMs could be recognized in 1985, 1997/1998, and 2003/2004 where the NAO index was negative or around zero (Figure 7b). This relationship between the DCM and the NAO was manifested in a significant correlation coefficient of the time coefficient of the first EOF and the winter NAO index with 0.37 ($p < 0.05$). The wavelet coherences between the time coefficient of the first EOF and the NAO showed the high correlation between

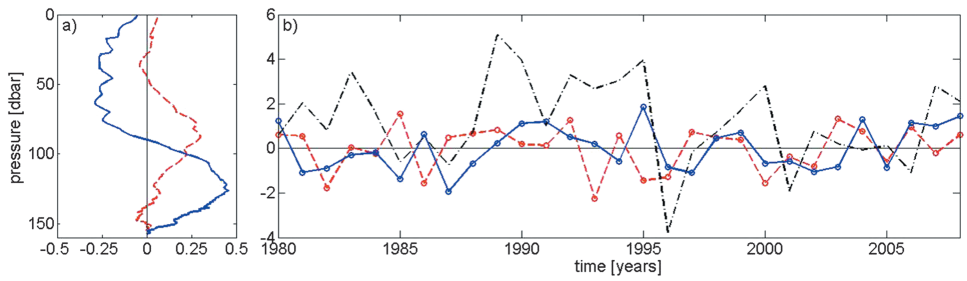

Figure 7. (a) The first (blue line) and second EOF (red dashed line) and (b) the time coefficients of the first EOF (blue line and circles) and second EOF (red dashed line and circles). Note that due to calculation with the standardized chlorophyll *a* hindcast, they have no units. Additionally, the winter NAO index is given (black dash-dotted line).

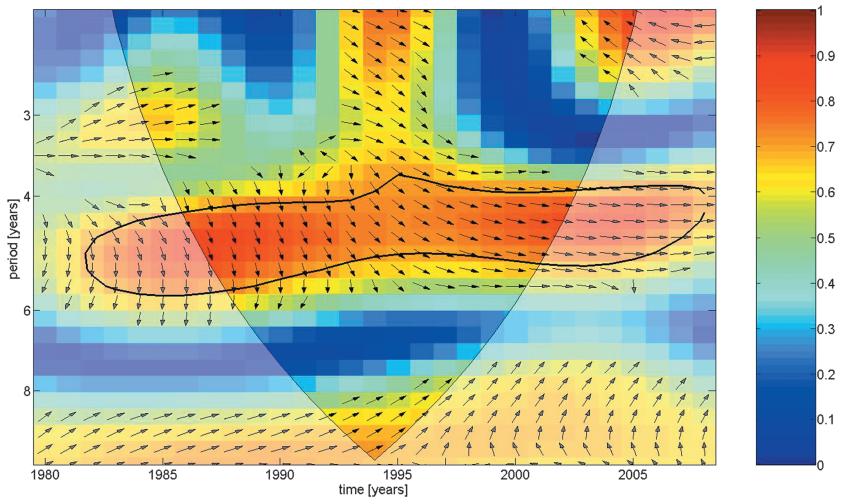

Figure 8. Wavelet coherence and phase between the winter NAO index and the time coefficient of the first EOF. Areas bordered by the black solid lines are within the 95% confidence level using the red noise model. The arrows indicate the phase difference (0° is given by a horizontal arrow pointing to the right, and an arrow pointing vertically upward means the time coefficient lags the NAO by 90°). The U-shaped curve shows limits of the cone of influence (COI). All signals outside COI are not statistically certain.

these two time series at periods between 4 and 6 years with a curling phase difference of 270° in the 1980s to no phase difference in the 2000s (Figure 8). This range of periods was previously reported by *Higuchi et al.* [1999] to be one of the dominant of the NAO. A correlation of the NAO on the same periods with no time lag was previously found with the current directions in the permanent thermocline in the Madeira Basin [*Fründt et al.*, 2013]. The initial phase difference of 270° would correspond to a leading of the chlorophyll *a* concentration to the NAO by about 1 year. The coherences were calculated by using annual mean values of the time coefficient of the first EOF as well as the annual winter NAO index (Figure 8). The time lag in the 1980s seemed to be biased by averaging, supposing a direct response with zero time lag for the 1980s, too. The NAO as dominant atmospheric pattern over the North Atlantic has high influence on the lateral wind field even in the horse latitudes where the study area is located [*Marshall et al.*, 2001; *Fründt and Waniek*, 2012]. Changes in the wind speed intensities cause different depths of the mixed layer which is correlated with the amount of nutrient supply into the euphotic zone and usually new production. The approximate zero time lag between the NAO and chlorophyll *a* concentration indicated that the primary production was sensitive to wind-induced changes of nutrient supply in the subsequent bloom.

An overlying long-term trend of the chlorophyll *a* concentration could not be detected within the studied time period. In the Madeira Basin, a temperature increase of 1.4 K was measured in 240 m between 1980 and 2008 [*Fründt et al.*, 2013]. Increasing ocean temperatures are predicted to cause a higher stratification which prevents nutrient input from below the euphotic zone leading to a decrease in phytoplankton growth [e.g., *Bopp et al.*, 2001; *Sarmiento et al.*, 2004; *Polovina et al.*, 2008; *Irwin and Oliver*, 2009]. However, the warming trend in 240 m was higher than the reported trends in sea surface temperature [*Denman et al.*, 2007] which would rather lead to destratification than enhanced stratification. *Dave and Lozier* [2013] found the same trend of faster warming of the deeper levels than the surface. Therefore, our study can neither verify the hypothesis of decreasing phytoplankton productivity with increasing stratification nor the results by *Lozier et al.* [2011] and *Dave and Lozier* [2013] who reported no correlation of stratification and primary production on interannual time scales, because the in situ measured time series of temperature in 240 m did not allow to make estimations of the stratification variability on interannual time scales. In our study, no correlation between long-term temperature trends and chlorophyll *a* concentration was found. A change in species composition due to rising temperatures was found in the Northeast Atlantic as well as the North and Baltic Seas [*Beaugrand et al.*, 2002; *Daufresne et al.*, 2009]. However, the introduced method cannot distinguish between different phytoplankton species and therefore the influence of rising temperatures on species size and composition could not be determined.

The observed period was characterized by a predominantly positive NAO as well as Atlantic Multidecadal Oscillation (AMO) gradient after the regime shift 1976–1981 [*Graham*, 1994; *Trenberth and Hurrell*, 1994]. Further studies are necessary to determine if the correlation between NAO and chlorophyll *a* concentration resists even in a state of decreasing AMO. Regarding the standardized chlorophyll *a* field (Figure 4b), the primary production seemed to be higher in the 1980s and the 2000s than in the 1990s. This probable variability with a period of approximately 20 years was too long to make any statistic significant statements especially in relation to low-frequency climate indices yet. Further studies will focus on the multidecadal variability of primary production and probable forcing mechanisms by the atmosphere and the ocean in the subtropical Northeast Atlantic over the entire last century, especially emphasizing the impact of the beginning of global warming in the last decades.

6. Summary

We introduced a method to reconstruct the chlorophyll *a* distribution over past decades based on occasional in situ measurements of temperature, nitrate, and chlorophyll *a*. It is applicable as a simple technique with low computational cost. Although in this work the chosen study area was the Madeira Basin, the method can be adapted to other regions of the global ocean as long as in situ data enabling the analysis of short- and long-term variability of primary production is available. By utilizing full-length modeled data sets (e.g., SODA POP 1871–2008), our method allows primary production to be studied in the context of low-frequency climate indices or twentieth century temperature changes, particularly as a comparison between the time periods before and during the warming currently taking place in wide areas of the global ocean. This will extend the results of the interannual influence of the NAO found in this study by a focus on the multidecadal variability. Moreover, the estimation of carbon uptake related to primary production can be extended to large oceanic regions. Application of the method described herein will provide essential information on the long-term variability of carbon uptake as response to changing climate conditions.

Acknowledgments

The authors thank all colleagues involved in obtaining the in situ measurements since 1989, the crews, and masters of the research vessels. The in situ measurements of temperature and nitrate are available at the Pangaea database (http://www.pangaea.de/). The SODA-POP temperature data are available on http://apdrc.soest.hawaii.edu/datadoc/soda_2.1.6.php. This work is financially supported by DFG (contract WA2157/5-1).

References

Antoine, D., and A. Morel (1996), Oceanic primary production, 1. Adaption of a spectral light-photosynthesis model in view of application to satellite chlorophyll observations, *Global Biogeochem. Cycles*, *10*, 43–55.

Beaugrand, G., P. C. Reid, F. Ibañez, J. A. Lindley, and M. Edwards (2002), Reorganization of North Atlantic marine copepod biodiversity and climate, *Science*, *296*, 1692–1694.

Behrenfeld, M. J., and P. G. Falkowski (1997), Photosynthetic rates derived from satellite-based chlorophyll concentration, *Limnol. Oceanogr.*, *42*(1), 1–20.

Behrenfeld, M. J., R. T. O'Malley, D. A. Siegel, C. R. McClain, J. L. Sarmiento, G. C. Feldman, A. J. Milligan, P. G. Falkowski, R. M. Letelier, and E. S. Boss (2006), Climate-driven trends in contemporary ocean productivity, *Nature*, *444*, 752–755.

Bopp, L., P. Monfray, O. Aumont, J.-D. Dufresne, H. Le Treut, G. Madec, L. Terray, and J. C. Orr (2001), Potential impact of climate change on marine export production, *Global Biogeochem. Cycles*, *15*(1), 81–99.

Boyce, D. G., M. R. Lewis, and B. Worm (2010), Global phytoplankton decline over the past century, *Nature*, *466*, 591–596.

Boyce, D. G., M. R. Lewis, and B. Worm (2011), Boyce et al. reply, *Nature*, *472*, E8–E9.

Carton, J. A., and B. S. Giese (2008), A reanalysis of ocean climate using Simple Ocean Data Assimilation (SODA), *Mon. Weather Rev.*, *136*, 2999–3017, doi:10.1175/2007MWR1978.1.

Carton, J. A., B. S. Giese, and S. A. Grodsky (2005), Sea level rise and the warming of the oceans in the Simple Ocean Data Assimilation (SODA) ocean reanalysis, *J. Geophys. Res.*, *110*, C09006, doi:10.1029/2004JC002817.

Chavez, F. P., M. Messié, and J. T. Pennington (2011), Marine primary production in relation to climate variability and change, *Annu. Rev. Mar. Sci.*, *3*, 227–260.

Dave, A. C., and M. S. Lozier (2010), Local stratification control of marine productivity in the subtropical North Pacific, *J. Geophys. Res.*, *115*, C12032, doi:10.1029/2010JC006507.

Dave, A. C., and M. S. Lozier (2013), Examining the global record of interannual variability in stratification and marine productivity in the low-latitude and mid-latitude ocean, *J. Geophys. Res. Oceans*, *118*, 3114–3127, doi:10.1002/jgrc.20224.

Daufresne, M., K. Lengfellner, and U. Sommer (2009), Global warming benefits the small aquatic ecosystems, *Proc. Natl. Acad. Sci. USA*, *106*, 12,788–12,793.

Denman, K. L., et al. (2007), Couplings between changes in the climate system and biogeochemistry, in *Climate Change: 2007: The Physical Science Basis. Contribution of Working Group I to the Fourth Assessment Report of the Intergovernmental Panel on Climate Change*, edited by S. Solomon et al., Cambridge Univ. Press, Cambridge, U. K., and New York.

Field, C. B., M. Behrenfeld, J. T. Randerson, and P. Falkowski (1998), Primary production of the biosphere: Integrating terrestrial and oceanic components, *Science*, *281*, 237–240.

Fründt, B., and J. J. Waniek (2012), Impact of the Azores front propagation on deep ocean particle flux, *Cent. Eur. J. Geosci.*, *4*, 531–544.

Fründt, B., T. J. Müller, D. E. Schulz-Bull, and J. J. Waniek (2013), Long-term changes in the thermocline of the subtropical Northeast Atlantic (33°N, 22°W), *Prog. Oceanogr.*, *116*, 246–260.

Fründt, B., J. W. Dippner, and J. J. Waniek (2015), Chlorophyll a reconstruction from in situ measurements: 2. Marked carbon uptake decrease in the last century, *J. Geophys. Res. Biogeosci.*, *120*, 246–253, doi:10.1002/2014JG002691.

Graham, N. E. (1994), Decadal scale climate variability in the tropical and North Pacific during the 1970s and 1980s: Observations and model results, *Clim. Dyn.*, *10*, 135–162.

Grasshoff, K., K. Kremling, and M. Ehrhardt (1999), *Methods of Seawater Analysis*, Wiley-VCH, Weinheim, Germany.
Gregg, W. W., and N. W. Casey (2004), Global and regional evaluation of the SeaWiFS chlorophyll data set, *Remote Sens. Environ.*, *93*, 463–479.
Grinsted, A., J. C. Moore, and S. Jevrejeva (2004), Application of the cross wavelet transform and wavelet coherence to geophysical time series, *Nonlinear Process. Geophys.*, *11*, 561–566.
Higuchi, K., J. Huang, and A. Shabbar (1999), Wavelet characterization of the North Atlantic Oscillation variation and its relationship to the North Atlantic sea surface temperature, *Int. J. Climatol.*, *19*, 1119–1129.
Hurrell, J. W. (1995), Decadal trends in the North Atlantic Oscillation: Regional temperatures and precipitation, *Science*, *269*, 676–679.
Irwin, A. J., and M. J. Oliver (2009), Are ocean deserts getting larger?, *Geophys. Res. Lett.*, *36*, L18609, doi:10.1029/2009GL039883.
Irwin, B. (2000), *Nutrient data from the Atlantic. JGOFS Canada data sets 1989–1998, CD-ROM version 1.0 Dec. 2000*, Mar. Environ. Data Serv., Dept. of Fisheries and Oceans, Canada. [Available at http://store.pangaea.de/Projects/JGOFS/Canada/home/datasets/irwin/readme.htm.]
Kirk, J. T. O. (2011), *Light and Photosynthesis in Aquatic Ecosystems*, 3rd ed., 665 pp., Cambridge Univ. Press, New York.
Legates, D. R., and G. J. McCabe Jr. (1999), Evaluating the use of "goodness-of-fit" measures in hydrologic and hydroclimatic model validation, *Water Resour. Res.*, *35*, 233–241.
Levitus, S., J. I. Antonov, and T. P. Boyer (2005), Warming of the world ocean, 1955–2003, *Geophys. Res. Lett.*, *32*, L02604, doi:10.1029/2004GL021592.
Levitus, S., J. I. Antonov, T. P. Boyer, R. A. Locarnini, H. E. Garcia, and A. V. Mishonov (2009), Global ocean heat content 1955–2008 in light of recently revealed instrumentation problems, *Geophys. Res. Lett.*, *36*, L07608, doi:10.1029/2008GL037155.
Lozier, M. S., A. C. Dave, J. B. Palter, L. M. Gerber, and R. T. Barber (2011), On the relationship between stratification and primary productivity in the North Atlantic, *Geophys. Res. Lett.*, *38*, L18609, doi:10.1029/2011GL049414.
Livezey, R. E. (1995), The evaluation of forecast, in *Analysis of Climate Variability*, edited by H. von Storch and A. Navarra, pp. 177–196, Springer, Berlin.
Mackas, D. L. (2011), Does blending of chlorophyll data bias temporal trend?, *Nature*, *472*, E4–E5.
Marshall, J., Y. Kushnir, D. Battisti, P. Chang, A. Czaja, R. Dickson, J. Hurrell, M. McCartney, R. Saravanan, and M. Visbeck (2001), North Atlantic climate variability: Phenomena, impacts and mechanisms, *Int. J. Climatol.*, *21*, 1863–1898.
McClain, C. R. A. (2009), A decade of satellite ocean color observations, *Annu. Rev. Mar. Sci.*, *1*, 19–42.
McQuatters-Gollop, A., et al. (2011), Is there a decline in marine phytoplankton?, *Nature*, *472*, E6–E7.
Mienert, J., G. Graf, C. Hemleben, K. Kremling, O. Pfannkuche, and D. E. Schulz-Bull (1998), *Nordatlantik 1996, Cruise No. 36, 6 June 1996–4 November 1996*, vol. 98-2, 320 pp., Meteor-Berichte, Leitstelle Meteor, Institut für Meereskunde der Universität Hamburg.
Mills, M. M., C. Ridame, M. Davey, J. La Roche, and R. J. Geider (2004), Iron and phosphorus co-limit nitrogen fixation in the eastern tropical North Atlantic, *Nature*, *429*, 292–294.
Nash, J. E., and J. V. Sutcliffe (1970), River flow forecasting through conceptual models, I. A discussion of principles, *J. Hydrol.*, *10*, 282–290.
Polovina, J. J., E. A. Howell, and M. Abecassis (2008), Ocean's least productive waters are expanding, *Geophys. Res. Lett.*, *35*, L03618, doi:10.1029/2007GL031745.
Protocols for the Joint Global Ocean Flux Study (JGOFS) core measurements (1994), Manual and Guides, 29, 97–100.
Rommets, J., R. Dapper, and H. J. W. de Baar (1991a), JGOFS North Atlantic R.V. Tyro Leg 1 of the cruise in 1989, Upper Ocean Processes, *NIOZ-RAPPORT, 1991-1*, Netherlands Institute for Sea Research (NIOZ), Texel, Netherlands, 27 pp., hdl:10013/epic.
Rommets, J., R. Dapper, and H. G. Fransz (1991b), JGOFS North Atlantic R.V. Tyro Leg 3 of the cruise in 1990, Upper Ocean Processes, *NIOZ-RAPPORT, 1991-3*, Netherlands Institute for Sea Research (NIOZ), Texel, Netherlands.
Rykaczewski, R. R., and J. P. Dunne (2011), A measured look at ocean chlorophyll trends, *Nature*, *472*, E5–E6.
Saba, V. S., et al. (2010), Challenges of modeling depth-integrated marine primary productivity over multiple decades: A case study at BATS and HOT, *Global Biogeochem. Cycles*, *24*, GB3020, doi:10.1029/2009GB003655.
Sarmiento, J. L., et al. (2004), Response of ocean ecosystems to climate warming, *Global Biogeochem. Cycles*, *18*, GB3003, doi:10.1029/2003GB002134.
Sathyendranath, S., T. Platt, E. P. W. Horne, W. G. Harrison, O. Ulloa, R. Outerbridge, and N. Hoepffner (1991), Estimation of new production in the ocean by compound remote sensing, *Nature*, *353*, 129–133.
Schwab, C., H. Kinkel, M. Weinelt, and J. Repschläger (2012), Coccolithophore paleoproductivity and ecology response to deglacial and Holocene changes in the Azores Current System, *Paleoceanography*, *27*, PA3210, doi:10.1029/2012PA002281.
Torrence, C., and G. P. Compo (1998), A practical guide to wavelet analysis, *Bull. Am. Meteorol. Soc.*, *79*, 61–78.
Trenberth, K. E., and J. W. Hurrell (1994), Decadal atmospheric ocean variations in the Pacific, *Clim. Dyn.*, *9*, 303–319.
Uitz, J., H. Claustre, A. Morel, and S. B. Hooker (2006), Vertical distribution of phytoplankton communities in open ocean: An assessment based on surface chlorophyll, *J. Geophys. Res.*, *111*, C08005, doi:10.1029/2005JC003207.
von Storch, H., and F. W. Zwiers (1999), *Statistical Analysis in Climate Research*, Cambridge Univ. Press, New York.
Waniek, J. (2010), *Cruise Report R.V. Poseidon Cruise No.: 404 [POS404] IOW*, 15 pp., GEOMAR, Warnemünde, Germany, doi:10.3289/CR_POS404.